A tunable Si3N4 integrated true time delay circuit for optically-controlled K-band radio beamformer in satellite communication

A Tunable Si_3N_4 Integrated True Time Delay Circuit for Optically-Controlled K-Band Radio Beamformer in Satellite Communication

N. M. Tessema, Z. Cao, J. H. C. Van Zantvoort, K. A. Mekonnen, A. Dubok, E. Tangdiongga, A. B. Smolders, and A. M. J. Koonen

***Abstract*—In this paper we present the design, realization, and experimental characterization of a photonic integrated true time delay circuit on a CMOS-compatible Si_3N_4 platform. The true time delay circuit consists of an optical side band filter for single side band modulation and an optical ring resonator for broadband time delay. Two methods of optical delay tuning are investigated: 1) optical wavelength and 2) thermo-optic delay tuning. The wavelength controlled tuning enables a large delay tuning range and can be done remotely from a distant location. The close to a linear phase measurements can be used for full beam-scanning of radio signals with frequencies in the 20 GHz band. The thermal control results in a 5 GHz RF delay bandwidth. A proof-of-concept 2 × 1 beamforming is demonstrated in the 20 GHz band. The design presented here can be employed to realize multi-beams for multi-users serviced by multiple satellites.**

***Index Terms*—Beam squint, focal plane array (FPA), free spectral range (FSR), Mach-Zehnder interferometer (MZI), off -resonance delay tuning, optical ring resonator (ORR), photonic integrated circuit (PIC), radio beamforming, wavelength delay tuning.**

I. Introduction

RADIO beamforming is the ultimate solution to satisfy the increased spatial bandwidth demand of wireless communication users. Beamforming, typically done by coherent combination of signals via multiple antenna elements, increases the power budget of a radio communication link. Electronic beamformers using traditional phase shifters have intrinsic narrowband characteristics which results in beam squinting and a reduced antenna gain for broadband RF signals. This is due to the constant phase shift applied for all frequency components of the signal. Wideband electronic beamformers based on true time delay (TTD) circuits can reduce problems associated with the beam squint; however, their bulky size, high power consumption and limitations at high radio frequencies pose major implementation problems [1]–[5]. Optically-controlled radio beamforming can provide a solution for the beam squint problem as a result of the enormous bandwidth provided by optical TTD devices. TTD provides a linear phase shift over a large frequency range. However, TTD devices made of bulky optics have limited applications due to their large size and large optical power losses. Therefore, the realization of photonic integrated TTD devices is the ultimate solution for wideband beamforming [3]–[5]. Further advantages of a photonic solution include reduced weight, compact size and immunity to electromagnetic interference [1]–[5].

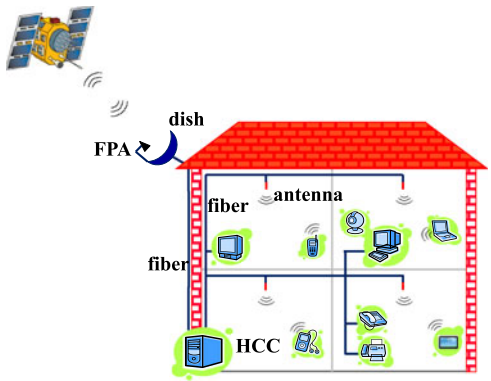

Fig. 1. Satellite-home commuication link with FPA antenna system (with photonic integrated beamformer circuit).

With the ever increasing demand for high capacity links, satellite-home communication is a key enabler technology especially in remote areas where a passive optical network infrastructure is not present. Fig. 1 shows such a satellite-home system in which an optically-controlled radio beamformer is integrated with the fiber in-home network. Within a home network, an optical fiber link can be used to provide wideband seamless connectivity to the devices in each room [6]. A focal plane array (FPA) antenna system operating in the 20 GHz radio frequency (RF) band receives and transmits RF signals to and from a satellite. Such an antenna system is comprised of a dish reflector fed by an array of antennas and can be controlled by electronic or optical beamforming. The FPA is mounted in the focal plane of the reflector antenna and serves as a feed (converts the received radio signal to electric current). This configuration

Manuscript received January 30, 2016; revised May 13, 2016 and June 17, 2016; accepted June 19, 2016. Date of publication June 26, 2016; date of current version September 25, 2016. This work was supported by the Dutch Science and Technology Foundation (STW) in the context of FREEBEAM project, and by the European Research Council (ERC FP7) in the context of BROWSE project.

N. M. Tessema, Z. Cao, J. H. C. Van Zantvoort, K. A. Mekonnen, E. Tangdiongga, and A. M. J. Koonen are with the Technical University of Eindhoven, COBRA Research Institute, Electro-optics Communication group, Electrical Eng. Department, 5600 MB Eindhoven, The Netherlands (e-mail: n.tessema@tue.nl; z.cao@tue.nl; J.H.C.v.Zantvoort@tue.nl; k.a.mekonnen@tue.nl; e.tangdiongga@tue.nl; a.m.j.koonen@tue.nl).

A. Dubok and A. B. Smolders are with the Technical University of Eindhoven, Centre for Wireless Communication, Electro magnetics group, Electrical Engineering Department, 5600 MB Eindhoven, The Netherlands (e-mail: a.dubok@tue.nl; a.b.smolders@tue.nl).

Color versions of one or more of the figures in this paper are available online at http://ieeexplore.ieee.org.

Digital Object Identifier 10.1109/JLT.2016.2585299

provides a high gain and beam-scanning over a limited angular scan range and achieves a better performance than traditional single-feed reflector antennas [7]. Since an FPA has more array elements than a traditional single feed reflector system, a higher equivalent isotropic radiated power level can be achieved [8]. Furthermore, it can be realized at much lower cost than a traditional phased array antenna. In this configuration, the antenna system can be aligned automatically via beamforming to receive signals from satellites. TTD based on Photonic Integrated Circuit (PIC) technology incorporated with the FPA antenna system can provide this beamforming functionality. The home communication controller (HCC) sends a control signal from a look-up table to tune the TTD PIC so that a radio beam can be pointed to a desired target satellite. Multiple wavelengths can be employed to generate multiple beams simultaneously. This allows satellite-home users to receive signals from multiple satellites at the same time. We designed, realized, and characterized TTD PIC beamformer intended to operate in such a satellite-home system.

Research and experimental work toward the implementation of the TTD PIC have been recently undertaken. A squint-free step-wise beam-steering PIC for indoor communications was demonstrated in an SOI platform [3]. It is based on a step-wise wavelength tunable TTD with arrayed waveguide grating feedback loop (AWG-L). A novel wavelength tunable step-wise 2D beam-steering system architecture for squint free operation is proposed in [4]. For beamforming purposes in satellite communication however, continuous tunability of a wideband optical delay is important for seamless beam scanning [5].

Previous experimental demonstrations of continuous TTD involved thermo-optic tuning. A thermally tunable Si_3N_4 TTD device that generates continuous delay for 2D beamforming based on optical ring resonators (ORR) has been reported in [9]. The device footprint is reduced by the introduced novel beamforming architecture. The same TTD unit is used to delay signals from a subarray at the increasing cost of one wavelength per subarray (a subarray is a single row of a 2-dimensional antenna array and it can be used to steer a beam in a single dimension). A TTD bandwidth of 8 GHz is achieved by cascading three ORRs, which increases the complexity of the device.

Reported works on TTD PIC beamformers were either solely based on thermo-optic continuous delay tuning or solely based on wavelength delay tuning with discrete delay values. In this paper, we present an experimental demonstration involving continuous delays based on *wavelength delay tuning* and continuous delays based on thermo-optic *off-resonant delay tuning* of the realized integrated TTD circuit.

The realized TTD circuit is a cascade of an optical side band filter (OSBF) and an ORR for broadband optical delay. The OSBF has a free spectral range (FSR) of 0.48 nm and is designed for single side band (SSB) operation. The SSB modulation relaxes the TTD bandwidth requirement of the ORR. To the best of our knowledge, so far, it is the most compact of all OSBF devices fabricated on a Si_3N_4 platform and has the largest FSR. Previous designs of OSBF reported in [9], [11], and [12] were limited to an FSR value of less than 0.2 nm. This enables our PIC beamforming operation in the 20 GHz RF band.

In order to enhance the footprint scalability of a TTD device for a large antenna array, two feasible approaches can be followed. Firstly, by increasing the TTD bandwidth per delay unit, it is no longer necessary to cascade delay units, thus the device footprint can be reduced, thereby keeping the device complexity to a minimum. We investigated this method in the *off-resonant delay tuning* technique presented in this paper. Secondly, by generating wavelength dependent delays, it is possible to use wavelength division multiplexing (WDM) to generate multiple delays per delay unit. This principle can be used to realize beamforming of large sized 2D antenna array, while keeping size and complexity of the TTD considerably low. By injecting N wavelengths into a single delay unit, N delays can be generated simultaneously. Thus, the required number of delay units decreases as the inverse of the number of wavelengths N; for instance, N can be chosen to be equal to the number of antenna elements in a subarray. As part of the TTD, wavelength (de)multiplexers need to be incorporated. The limitation of the WDM optical beamforming approach is that a large antenna array needs a large number of lasers. A WDM optical beamforming technique that decreases the number of the required light sources is proposed in [13]. A combination of dispersive and non-dispersive delays with discrete components was used to generate multiple delays with a single wavelength, thereby reducing the number of required lasers. Implementation of this principle in a PIC can lead to a compact WDM beamformer for 2D antenna arrays. Furthermore, WDM approach can be extended to generate multiple beams by using a single wavelength per beam. The *wavelength delay tuning* technique presented in this paper can be employed in these cases. It also provides with a passive and remote beam-steering control.

This paper is an extension of our paper given in [14]. The novelty of this paper lies from the fact that the TTD circuit is tailored for K-band RF signals and two unique delay tuning methodologies: *off-resonant delay tuning* for broadband delay and *wavelength delay tuning* for remote and passive beam-steering control are investigated and experimentally verified. Both delay tuning methods are based on a single ORR per delay unit, thus a reduced device complexity and footprint of the TTD is achieved compared to what has been presented in [9], [11].

The *wavelength delay tuning* was demonstrated to provide full scanning of the radio beams with a TTD bandwidth up to 2 GHz. A broadband delay with instantaneous TTD bandwidth of 5 GHz is demonstrated using the *off-resonant delay tuning*. A fine-tuning of the broadband delay at the off-resonance wavelengths is accomplished thermo-optically, and enables scanning angles ranging from –28° to 34° for a 19.5 GHz signal. An experimental demonstration on a proof-of-concept, 2×1 beamformer based on the TTD PIC for a coherent combination of the beamformer channels is presented. Since the fabrication of the FPA is undergoing, the integration of TTD with FPA for beamforming experiments will be included as part of our future work.

The rest of the paper is organized as follows. Section II describes the basic theoretical principles of optically-controlled radio beamforming. Section III describes the design, realization, and operational principle of the TTD circuit. Section IV describes about the *wavelength delay tuning* and *off-resonant*

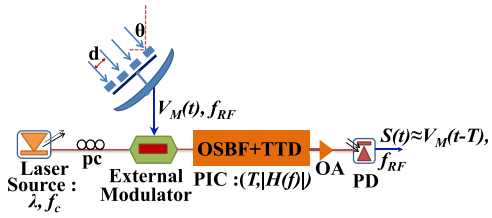

Fig. 2. Schematic of optically-controlled radio beamformer system.

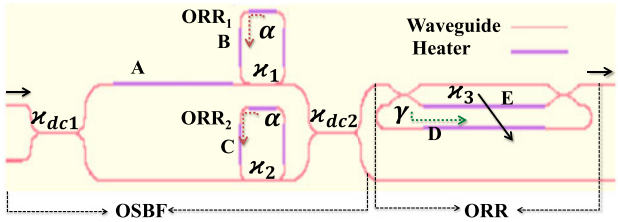

Fig. 3. Schematic diagram of the TTD device (cascade of OSBF and ORR).

delay tuning methods in an ORR. Experimental setup, characterization results and discussions are given in Section V, and conclusions follow in Section VI.

II. Theoretical Principles

This section describes the theoretical principles behind the presented optically-controlled radio-beamformer. In an optically-controlled radio beamformer, an RF signal received from an FPA modulates the light signal as shown in Fig. 2. An optically-controlled TTD enables beamforming/steering. The tunable laser source emits the electric field E_0 at the frequency f_c. $V_M(t)$ is the modulating signal from the M^{th} antenna element at frequency f_{RF}. The output of the Mach-Zehnder modulator for a modulation index m can be written as in (1) for a modulator bias condition when no higher-order harmonics are present

$$E = E_0\,[1 + m\,V_M\,(t)]\,e^{j2\pi f_c t}. \tag{1}$$

After the signal passes through the optical TTD, we obtain the expression of (2), where $|H(f)|$ is the magnitude response of the TTD chip and T represents the delay value at which the TTD is tuned

$$E = E_0\,|H(f)|[1 + m\,V_M(t - T)]e^{j2\pi f_c (t-T)}. \tag{2}$$

After photo detection, the recovered electrical signal $S(t)$ can be written as in (3) which is the delayed version of the antenna signal. In (3), γ is the responsivity of the photodetector and β represents the magnitude gain of the optical system

$$S\,(t) = \beta\gamma|H\,(f)|^2 E_0{}^2 V_M\,(t - T)\,. \tag{3}$$

By combining the delayed signal with un-delayed reference signal, a simple beamformer can be steered. It is obvious from (3) that by tuning the value of the optical delay T it is possible to scan the desired steering angle θ of the antenna array. The delay and the steering angle are related as $T = d\sin\theta/c$, where d is inter-element antenna spacing and c is the speed of light.

In addition to the tunability of the TTD value T, the instantaneous bandwidth in which T is constant is also important. It avoids the problem of beam squint. It determines how much phase error is introduced by the beamforming system. The phase error is the result of the phase response deviation from linearity. The achievable TTD bandwidth of an integrated device based on an ORR is correlated with its FSR; the larger the FSR, the larger the TTD bandwidth. Conversely, the round trip delay of the device decreases as FSR increases. The minimum bending radius required to avoid bending losses limits the FSR. Therefore, to relax the TTD bandwidth requirement, single sideband modulation (SSB) is implemented. Thus, an OSBF is an integral part of the TTD device presented in this paper.

Furthermore, the frequency dependent amplitude response $|H(f)|$ of the TTD can result in an undesired amplitude weighting (beam shaping), when two or more beamforming channels are tuned at different wavelengths. The desired beam shaping can be achieved by using controlled amplitude weighting using optical tunable power couplers, or variable gain electrical amplifiers.

III. Design, Realization, and Operational Principles

The designed TTD beamformer is a cascade of a thermally tunable OSBF for a single sideband operation and a delay unit based on a thermally tunable ORR. OSBF enables SSB operation, thereby relaxing the TTD bandwidth requirement in the ORR. The schematic diagram of the TTD device is shown in Fig. 3. It occupies a wafer space of 2×11 mm^2. The transfer function of TTD beamformer, H is the product of the transfer function of the OSBF, H_{OSBF} and the transfer function of the ORR, H_{ORR} as given in (4).

$$H\ = H_{OSBF}\ *\ H_{ORR} \tag{4}$$

The OSBF is designed for RF signals in the frequency range from 20–40 GHz. It is based on a second-order butterworth filter. It is implemented as a double ring assisted Mach-Zehnder interferometric structure and it is illustrated in Fig. 3. It occupies a small footprint of 2×6 mm^2 due to the compact design of loaded ORRs. The Mach-Zehnder interferometer (MZI) arms are made of two 3 dB directional couplers, in which connecting waveguides are loaded with ORRs (ORR_1 and ORR_2). Three thermo-optic shifters enable re-configurability and wavelength tunability of the filter response. The compact ORRs loaded in the MZI arms have an FSR of 60 GHz. A compact ring layout with a single fixed coupler was employed which reduced the round trip length of ORR_1 and ORR_2 to 5 mm and resulted in a compact OSBF with an FSR of 60 GHz. The implementation of the fixed couplers with an asymmetric layout (one parallel waveguide is made straight) further promoted a compact implementation of the OSBF. To the best of our knowledge, it is a device with the largest FSR of the filters fabricated in a Si_3N_4 platform. The response of the OSBF is written as in (5), where T_1 is the round trip of ORR_1 and T_2 is the round trip of ORR_2, $\varkappa_1$ and $\varkappa_2$

TABLE I
DESIGN PARAMETERS

Parameter	Values
$\varkappa_{dc1}$	0.5
$\varkappa_{dc2}$	0.5
$\varkappa_1$	0.4
$\varkappa_2$	0.4
Heater lengths (μm) [A,B,C,D,E]	[2000, 1365, 1365, 2000, 2000]
FSR of ORR(GHz)	26.5
FSR of OSBF(GHz)	60
TTD Wafer area (mm^2)	2×11
OSBF Wafer area (mm^2)	2×6
ORR Wafer area (mm^2)	2×5

are the corresponding coupling coefficients, α is the amplitude transmission coefficient of the feedback loops of ORR_1 and ORR_2

$$H_{OSBF} = e^{-j\phi_A} * H_{ORR,1} * H_{ORR,2}$$
$$H_{ORR,1} = \frac{\sqrt{1-\varkappa_1} - \alpha e^{-j2\pi f T_1} \; e^{-j\phi_B}}{1 - \sqrt{1-\varkappa_1}\alpha e^{-j2\pi f T_1} \; e^{-j\phi_B}}$$
$$H_{ORR,2} = \frac{\sqrt{1-\varkappa_2} - \alpha e^{-j2\pi f T_2} \; e^{-j\phi_C}}{1 - \sqrt{1-\varkappa_2}\alpha e^{-j2\pi f T_2} \; e^{-j\phi_C}} \quad (5)$$

ϕ_A, ϕ_B, and ϕ_C are heater induced phase shifts at heaters A, B, and C respectively.The rejection ratio of the filter is tuned by changing the value of ϕ_A. The width of the pass band or the rejection can be varied by detuning ORR_1 and ORR_2.The ORR delay unit which is shown in Fig. 3 is implemented using a tunable MZI structure for tuning coupling coefficent $\varkappa_3$. The transfer function of the ORR is given in (6), γ is the corresponding amplitude transmission coefficient, and T_3 is the round trip time of ORR. It is seen from (6) that the coupling coefficient $\varkappa_3$ of the tunable MZI coupler is tuned by changing the phase of heater E, ϕ_E. Tuning the coupling coefficent enables tuning of the quality factor and therefore tuning of the group delay profile. The generated optical delay of an ORR is given in (7),where ψ_{ORR} is the phase response of the ORR. The design parameters of the TTD are summarized in Table I

$$H_{ORR} = \frac{\sqrt{1-\varkappa_3} - \gamma e^{-j2\pi f T_3} \; e^{-j\phi_D}}{1 - \sqrt{1-\varkappa_3}\gamma e^{-j2\pi f T_3} \; e^{-j\phi_D}},$$
$$\varkappa_3 = \cos^2 \phi_E \quad (6)$$
$$T_{ORR} = \frac{-d\,(\psi_{ORR})}{d\,(\phi)}. \quad (7)$$

The realized beamformer chip under a visible light test is shown in Fig. 4. The chip occupies an area of 16×16 mm^2. In addition to the beamforming TTD, it contains test structures of the ORR, and the OSBF. It is fabricated in a CMOS compatible Si_3N_4 platform incorporating moderate index contrast. The minimum bending radius value of 125 μm used in all structures of the bent waveguides ensures that bending losses are minimized. A double stripe waveguide design, in which the core layer is a SiO_2 layer sandwiched between two Si_3N_4 layers is used. A detailed description of the fabrication process of a double stripe Si_3N_4 waveguide is found in [10]. The thermo-optic phase shifters are realized by depositing a layer of chromium on top of the optical waveguides. Thermal crosstalk between the heaters is avoided by keeping a gap of 250 μm between any two heating elements. Lead wires made of chromium and gold facilitate electrical connections to the heater elements. The PIC is provided with spot size converters at input and output ports in which a vertical tapering of the Si_3N_4 layer is made to match with the mode profile of a single mode fiber (SMF28). The spot-size converters are designed to only couple TE polarized light into the optical chip. The initial operational voltage setting of the TTD is determined by the frequency of the RF signal. Accordingly, the pass bandwidth of the TTD is tuned by optimizing the heater voltages of A, B, and C while maintaining rejection ratios of 20 dBs and higher on the lower sideband. Resonance wavelength shifting of the ORR response is carried out by tuning of the heater voltage D. The delay profile is varied by changing the voltage applied on heater E.

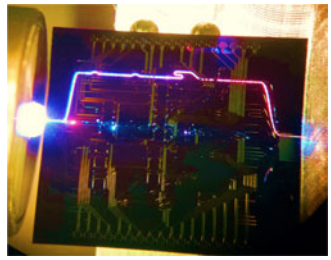

Fig. 4. Realized chip under visible light test showing input-output connectivity.

IV. DELAY TUNING METHODOLOGIES

Typical ways of tuning the optical delay are changing the wavelength of the input light or changing the refractive index of the optical waveguide via thermo-optic tuning. We propose the wavelength and thermo-optic tuning of the continuous optical delay realized in a Si_3N_4 ORR. The temperature of the optical waveguides is varied via the resistive electrodes mounted on the top of the waveguides. The electrodes (heaters) convert the applied electrical energy into heat energy. The temperature-brought phase variation tunes the coupling ratio ($\varkappa_3$) of the ORR, which is a mechanism to thermo-optically tune the optical delay. Fig. 5 illustrates the theoretical group delay responses along with the calculated quality factors of the ORR shown in Fig. 3. The simulation is done based on (6) and (7), for the ORR design parameters given in Table I and coupling values $\varkappa_3$ ranging from 0.2 to 0.75. Group delay responses corresponding to lower coupling coefficient (high quality factor) exhibit a large peak group delay at the resonance wavelengths which drops to a very flat, small delay values at the off-resonance wavelengths. However, responses corresponding to high coupling coefficients (low quality factor) are characterized by bell shaped the delay profile across its FSR in which the gradient of delay is relatively smaller. The *quality factor* (Q) of the ORR can be thermo-optically tuned by changing the coupling ratio $\varkappa_3$ to optimize the TTD bandwidth.

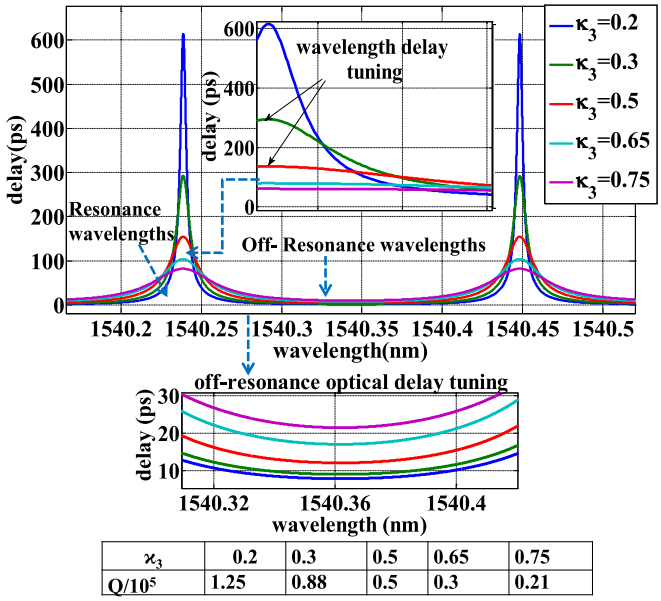

κ_3	0.2	0.3	0.5	0.65	0.75
Q/10^5	1.25	0.88	0.5	0.3	0.21

Fig. 5. Theoretical plot of delay response of an ORR, with wavelength delay tuing, and off-resonance delay tuning, calculated *quality factor* (Q).

A. Wavelength Delay Tuning

The wavelength control of the optical delays employs the wavelength dependent delay profile of the ORR as illustrated in a zoomed in picture (top) of Fig. 5. The variation of delay per unit wavelength is dependent on the quality factor of the ORR. For higher quality factors (lower coupling ratios, $\varkappa_3 = 0.2$), the group delay response is characterized by a very steep peak at the resonance wavelength and while being relatively flat at other wavelengths. This means there is a very large group delay variation in a small confined wavelength range, which limits the maximum achievable TTD bandwidth via wavelength tuning. Conversely, by tuning $\varkappa_3$ to 0.3, a larger TTD bandwidth can be realized due to smaller gradient of the delay per unit wavelength. By increasing $\varkappa_3$ further to 0.6, 0.65, and 0.75, the TTD bandwidth can be increased with less delay variation per unit wavelength. Therefore, the desired delay tuning range per wavelength can be optimized via tuning of $\varkappa_3$.

B. Off-Resonance Thermo-Optic Delay Tuning

Since the bandwidth-delay product for an ORR is constant, tuning at small delays results in a large TTD bandwidth. Therefore, by tuning at the off-resonance wavelengths as illustrated in a zoomed in picture (bottom) of Fig. 5, it is possible to maximize the TTD bandwidth per delay unit with a limited delay tuning range. This delay generation mechanism provides a large instantaneous TTD bandwidth per single ORR without increasing the design complexity.

In our earlier work, we have presented an experimental demonstration of an off-resonance thermal tuning of a single ORR for an instantaneous TTD bandwidth of 5 GHz [15]. This delay generation mechanism is well suited for higher frequency RF signals (20 GHz and higher) where delay variation of few tens of picoseconds is enough to provide full beam-scanning.

V. Experimental Set Up, Results, and Discussion

The measurements were done by using the fiber-to-chip coupling set up shown in Fig. 6(a). A 16-fiber array unit (FAU) with a 127 μm pitch was used for the input and output coupling of the optical chip. DC probes were used to make electrical connections with contacts pads on the optical chip. The temperature of the optical chip was maintained at 20 °C using a Peltier based thermo-electric cooler (TEC). The end-to-end optical loss of 11 dB was measured across the chip. From voltage-current measurements, the resistance of the heaters is found to be 575 Ω, 383 Ω, 383 Ω, 575 Ω, and 575 Ω for heater A, B, C, D, and E respectively.

A. Phase Measurements

For phase measurements on the TTD device, the experimental setup shown in Fig. 6(b) is employed. The output of a vector network analyzer (VNA) of a radio signal is optically modulated and transmitted through the TTD. During the measurement the wavelength of the laser is changed or thermo-optic tuning of heater E is done to vary the delay of the ORR. The detected RF signal is fed back to the VNA and phase response measurements are retrieved. The RF phase response of the optical chip measured from the (VNA) is used to characterize the delay. The delays are measured against a minimum delay taken as a reference. Two delay tuning methods: *Wavelength delay tuning*, and *off-resonant delay tuning* are investigated. The voltage settings used for *Wavelength delay tuning* (Setting 1) and the *off-resonant delay tuning* (Setting 2) are given in Fig. 6(c). The double-side spectrum measured at the input of the TTD and the single-sideband spectrum at the output of the TTD are shown in Fig. 6(d). SSB modulation is enabled with a rejection ratio of 20 dB for a 19.5 GHz signal. The optical spectral responses of the TTD for the given voltage settings are provided in Fig. 6(e). It is to be noted that the spectrums have differing pass bandwidth due to different voltage settings.

1) Wavelength Delay Tuning: The *wavelength delay tuning* involves tuning the heater voltages for the desired filtering functionality and the ORR delay as stated in Setting 1. The measurement is then conducted by progressively varying the light wavelength in steps of 2 pm. The delays are obtained from the slope of the best linear fits of the measured phase responses. The deviation of the phase response from linearity is quantified as the root mean square (rms) phase error and rms delay error. In Table II, the phase slope of the linear fit in deg/GHz, the rms phase error in degrees, the delay in ps, and the rms delay error in ps at each of the measurement wavelengths are given. Fig. 7(a) and (b) show the phase measurements: the solid lines are the measurements and the dotted lines represent their best linear fits. First, the phase response measurement with bandwidth of 1 GHz as given in Fig. 7(a) is done while the wavelength was tuned from 1540.512 nm to 1540.526 nm and heater E voltage was tuned at 5 V. The measured delay values ranged from 252 ps to 34 ps. A nearly linear phase response was mea-

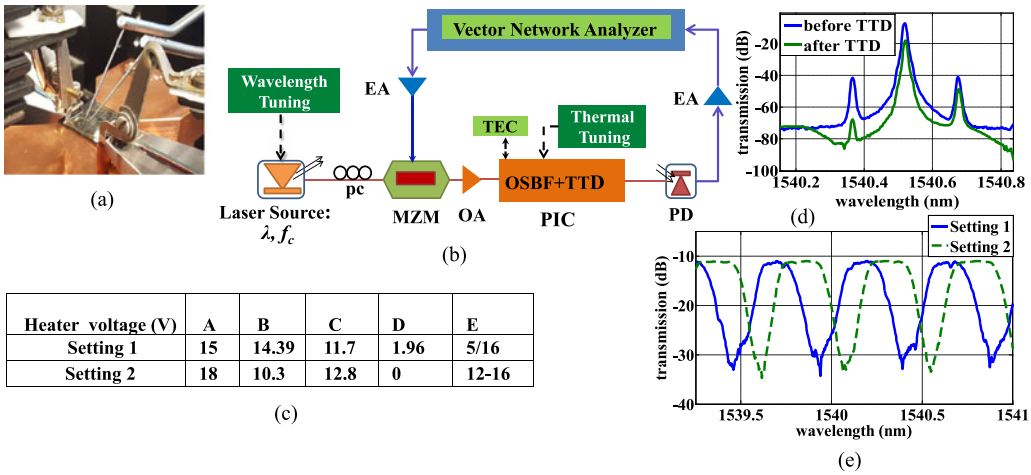

Heater voltage (V)	A	B	C	D	E
Setting 1	15	14.39	11.7	1.96	5/16
Setting 2	18	10.3	12.8	0	12-16

(c)

Fig. 6. (a) Photograph of fiber to chip-coupling, (b) experimental setup, (c) heater voltage settings (Setting 1 for wavelength tuning, and Setting 2 for thermo-optic tuning), (d) optical spectrum before the chip and after the chip (SSB modulation), (e) Spectrum measurement for *wavelength delay tuning* (Setting 1) and *off-resonant delay tuning* (Setting 2).

TABLE II
WAVELENGTH DELAY TUNING PARAMETERS

λ	wavelength (nm)	fitted phase slope (deg/GHz)	delay (ps)	rms delay error (ps)	rms phase error (deg)
λ_1	1540.512	90.9	252	3.9	1.42
λ_2	1540.514	72.8	202	6.2	2.24
λ_3	1540.516	54.8	152	5.9	2.11
λ_4	1540.518	40.4	112	4.5	1.63
λ_5	1540.520	29.2	81	3.5	1.27
λ_6	1540.522	20.8	58	2.3	0.85
λ_7	1540.524	15.2	42	1.4	0.5
λ_8	1540.526	12.2	34	1.1	0.4
λ_9	1552.61	47.4	131.7	2.3	1.63
λ_{10}	1552.62	47.3	132.2	2.3	1.62
λ_{11}	1552.63	49.5	137.4	2.2	1.61
λ_{12}	1552.64	54.7	151.9	2	1.5
λ_{13}	1552.65	63	174.8	1.6	1.17
λ_{14}	1552.66	71.6	198.8	1.7	1.28
λ_{15}	1552.67	73.5	204.2	3.3	2.35

sured, where the maximum rms delay error is 6.2 ps and the corresponding rms phase error is only 2.24°. The TTD bandwidth and its deviation from linearity could be improved by thermo-optic tuning of the quality factor as discussed in Section II. To do that, the heater E voltage was tuned to 16 V, and phase measurements for TTD bandwidth of 2 GHz as given in Fig. 7(b) was conducted, while wavelength was tuned from 1552.61 nm to 1552.67 nm. The delay values ranged from 131.7 ps to 204.2 ps. A better fit to linearity was achieved in this case, as the maximum rms delay error is only 2.3 ps. It is to be noted that the delay variation in this case is smaller because of smaller wavelength delay slope. The measured delays allow more than 2 π rad phase shift for RF frequencies in the 20 GHz band. This enables beam-scanning for any desired direction of a target satellite. Due to the periodic response of the ORR, each of the tuned delays can be generated after one FSR (0.21 nm).

2) Off-Resonance Thermo-Optic Delay Tuning: The wavelength is tuned at the off-resonance wavelength where the delay is flat and the tuning is done by progressively changing the voltage for heater E in steps of 0.2 V. The VNA is swept from 17–22 GHz. Fig. 7(c) shows the phase response measurements obtained when voltage values applied on heater E was varied from 12 to 16 V. It can be seen that the large degree of flatness at the off-resonance band resulted in a linear phase response. Accordingly, the measured delay values ranged from 31.1– 57.7 ps. The fine delay tuning ranges obtained using this technique were used to calculate the beam-scanning range at 19.5 GHz for a 2 $\times$ 1 beamformer, while taking the delay at 13.8 V as a reference. It is possible to realize steering angle in the range [–28° to 34°]. The calculation was done using the relation $\theta = \sin^{-1}[c\Delta T/d\,]$, where c is the speed of light, ΔT is the delay difference between the two channels. The delay for the reference channel was set at 43.3 ps, while the measured delay values were used for the delayed channel. The half-wavelength antenna spacing d of 0.77 cm was used since it corresponds with the largest delay needed to realize the given steering angles. This delay tuning method can be employed for bandwidth intensive applications.

B. Coherent Combination of a 2 $\times$ 1 Beamformer Channels

A proof-of-concept 2 $\times$ 1 beamformer made up of un-delayed path passing through a fiber (Ch_1) and a delayed path (Ch_2) passing the TTD circuit is shown in Fig. 8(a). An optical phase difference exists between channels due to different signal paths of the two channels after the 3 dB coupler. The tunable TTD is tuned to compensate the phase difference between the two channels for coherent combination. The two channels are put into separate PDs and are electrically combined with RF combiner. The input powers into the two PDs are balanced using variable optical attenuators (VOA) for equivalent detected RF power. Measurements of the RF power for the Ch_1, Ch_2 and the combined channel $Ch_1 + Ch_2$ is done while the local oscillator

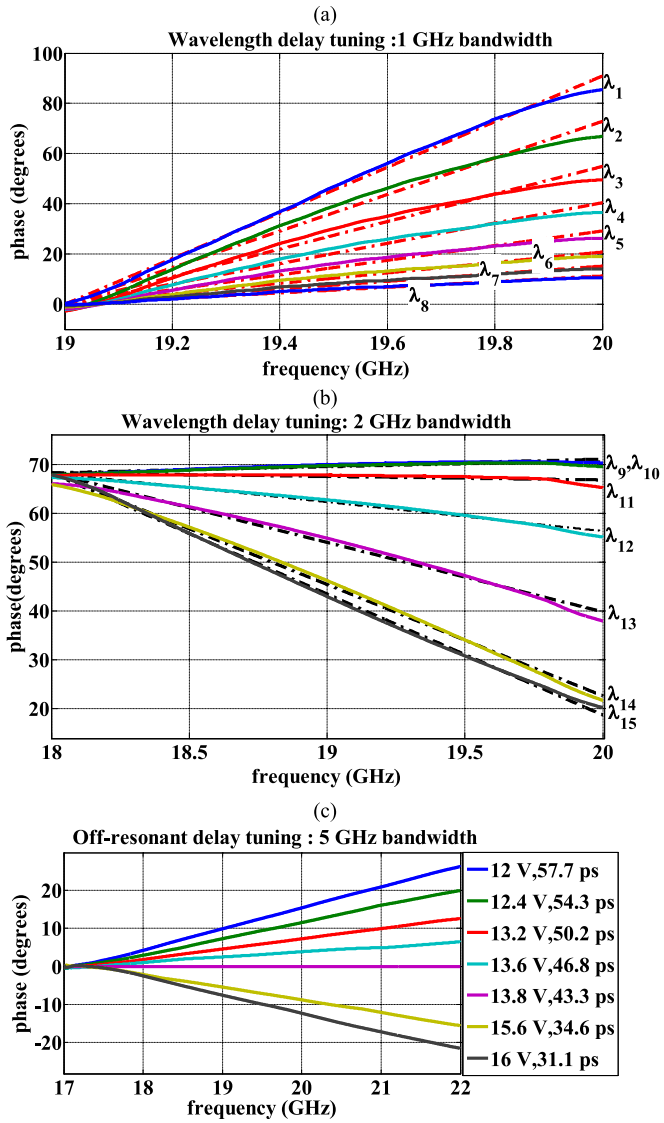

Fig. 7. Phase response measurements (a) *Wavelength delay tuning*: 1 GHz bandwidth (b) *Wavelength delay tuning:* 2 GHz bandwidth (c) *Off-resonant delay tuning:* 5 GHz bandwidth.

frequency is varied from 17.5–22.5 GHz. It can be seen that from Fig. 8(b) that a 6 dB increase in the RF power is achieved because of coherent combination the two channels. The roll-off in the received power measurements is the result of the fact that the PDs have a –3 dB bandwidth at 20 GHz. This proof-of-concept beamformer demonstrates the performance of the TTD for RF signals in the 20 GHz band.

VI. Conclusion

We have presented the design, realization, and experimental demonstration of an on-chip TTD for radio-satellite beamforming. The compact design of the TTD allows an RF beamforming in the 20 GHz frequency band. A proof-of-concept 2 × 1 beamformer based on a TTD PIC is demonstrated in the 20 GHz band. The device design is useful in satellite-home systems with radio beamforming.

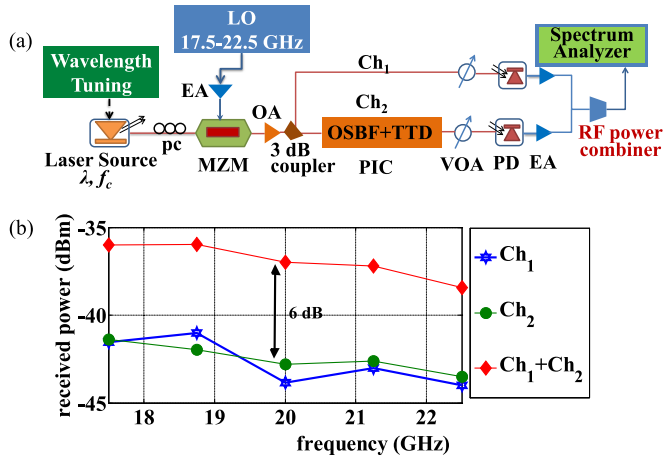

Fig. 8. (a) Experimental setup for coherent combination of a 2-by-1 beamformer (b) receive power of undelayed path: Ch_1, delayed path: Ch_2, combined channel: $Ch_1 + Ch_2$.

Measurement results indicate that the *wavelength delay tuning* method generates more than 2π rad of phase shift for RF signals in the 20 GHz band within a 2 GHz TTD bandwith, enabling beam pointing of the RF signals to any desired angle. The generation of wavelength dependent delays can be employed to demonstrate multi-beamforming by using a single wavelength per beam. Utilizing N wavelengths results in N simultaneous beams, hence multiple satellite links can be formed at once. Furthermore, remote control of the beamformer from a distant location is enabled via a *wavelength delay tuning*. Using thermo-optic delay tuning, a broadband delay for an instantaneous TTD bandwidth of 5 GHz is demonstrated. The measured delays enable steering ranges from –28° to 34° for RF signals at 19.5 GHz. In real applications, *off-resonant delay tuning* can be chosen for targets requiring fine-tuning of delay such as satellites in geostationary orbits. Alternatively, *wavelength delay tuning* can be used to provide delay values with larger variation, and the necessary delay fine-tuning can be accomplished by tuning wavelength or the coupling value.

Acknowledgment

The authors would like to acknowledge the technical support from Phoenix Software and SATRAX B.V.

References

[1] J. Capmany and D. Novak, "Microwave photonics combines two worlds," *Nature Photon.*, vol. 12, no. 5, pp. 319–330, 2007.
[2] Z. Cao, F. Li, H.P.A Van Den Boom, E. Tangdiongga, and A. M. J Koonen, "Optical true time delay microwave beam-steering with 1 Gbps wireless transmission for in building networks," in *Proc. Eur. Conf. Optical Commun.*, 2013, pp. 1–3.
[3] Z. Cao *et al.*, "An integrated step-wise optical tunable true-time-delay system for the microwave beam-steering towards in-home devices," in *Proc. Opto Electron. Commun. Conf.*, 2014, pp. 864–866.
[4] A. M. J. Koonen and Z. Cao, "Optically-controlled 2D radio beam-steering system," in *Proc. Int. Topical Meeting Microw. Photon. 9th Asia-Pacific Microw. Photon. Conf.*, 2014, pp. 389–391.
[5] D. Marpaung, C. Roeloffzen, R. Heideman, A. Leinse, S. Sales, and J. Capmany, "Integrated microwave photonics," *Laser Photon. Rev.*, vol. 7, pp. 506–538, 2013.

[6] A. M. J. Koonen and E. Tangdiongga, "Photonic home area networks," *IEEE J. Lightw. Technol.*, vol. 32, no. 4, pp. 591–604, Feb. 2014.
[7] A. Zamanifekri and A. B. Smolders, "Beam squint compensation in circularly polarized offset reflector antennas using a sequentially rotated focal-plane array," *IEEE L. Antennas Wireless Propag.*, vol. 14, pp. 815–818, Mar. 2015.
[8] A. Al-Rawi, A. Dubok, M. H. A. J. Herben, and A. B. Smolders, "Point-to-point radio link variation at E-band and its effect on antenna design," in *Proc. Progress In Electromagn. Res. Symp.*, 2015, pp. 1–5.
[9] M. Burla *et al.*, "Multi-wavelength-integrated optical beamformer based on wavelength division multiplexing for 2-D phased array antennas," *IEEE J. Lightw. Technol.*, vol. 32, no. 20, pp. 3509–3520, Oct. 2014.
[10] A. Leinse *et al.*, "TriPleX waveguide platform: Low-loss technology over a wide wavelength range," in *Proc. SPIE*, 2013, pp. 1–13.
[11] C. Roeloffzen *et al.*, "Silicon nitride microwave photonic circuits," *Opt. Express.*, vol. 21, no. 19, pp. 22937–22961, 2013.
[12] M. Burla, "Advanced integrated optical beamforming networks for broadband phased array antenna systems," Ph.D. dissertation, Univ. of Twente, Enschede, The Netherlands, 2013.
[13] B. Vidal *et al.*, "Simplified WDM optical beamforming network for large antenna arrays, " *IEEE Photon. Technol. Lett.*, vol. 18, no. 10, pp. 1200–1202, May 2006.
[14] N. Tessema, Z. Cao, A. Dubok, E. Tangdiongga, A. B. Smolders, and A. M. J. Koonen, "A Si_3N_4 PIC for optically-controlled 2D radio beamforming in satellite communications," in *Proc. Int. Topical Meeting Microw. Photon.*, 2015, pp.1–4.
[15] N. Tessema *et al.*, "Radio beam-steering via tunable Si_3N_4 optical delays for Multi-Gbps K-band satellite communication," in *Proc. Opt. Fiber Commun Conf.*, 2016, pp. 1–3.

Netsanet Tessema (S'14) received the B.Sc. degree in electrical engineering from Mekelle University, Ethiopia, in 2007 and worked at Ethio Telecom for the next 3 years. She received the M.Sc. degree from Delft University of Technology, The Netherlands. She has been working toward the Ph.D. degree at Eindhoven University of Technology, The Netherlands, since 2013. Her current research interests include photonic integration, radio over fiber and smart antenna systems.

Zizheng Cao (S'11) received the M.Eng. degree in telecom engineering from Hunan University, Changsha, China, in 2010. He received the Ph.D. degree (*Cum Laude*) from Eindhoven University of Technology, The Netherlands, in 2015. Since then, he has been working as a Postdoctoral Researcher at Eindhoven University of Technology. He received a Graduate Student Fellowship of IEEE Photonics Society in 2014. He holds two Chinese patents and one U.S. provisional patent. His research interests include integrated (microwave) photonics circuits, digital signal processing, and optical wireless communication.

Johan van Zantvoort received the Graduate degree in applied physics from the Technical College of Eindhoven, The Netherlands, in 1994. Since then, he was with DAF Trucks Research, Philips Centre for Manufacturing Technology, and Philips Novatronics. He is currently engaged in research on packaging technologies of integrated optical devices at the Eindhoven University of Technology. He is the (co)author of more than 50 refereed papers and conference contributions.

Ketemaw Mekonnen (S'15) received the B.Sc. degree in electrical engineering from Mekelle University, Ethiopia, in 2007. He received the double M.Sc. degree in the Erasmus Mundus Master on photonic networks engineering program from Scuola Superiore Sant'Anna, Italy, and Aston University, U.K., in 2013. He is currently working toward the Ph.D. degree in Eindhoven University of Technology, The Netherlands. His current research interests include dynamic optical routing, radio over fiber, signal processing, and optical wireless communication.

Aleksei Dubok (S'09) received the B.Sc. and M.Sc. degrees (Hons.) from Saint Petersburg State Electrotechnical University, Russia, in 2008 and 2010, respectively, and the second M.Sc. degree (Hons.) from Lappeenranta University of Technology, Finland, in 2011. From 2007 to 2010, he worked at TELROS Integration, Russia. In 2013, he received the professional doctorate in engineering degree from the Eindhoven University of Technology, The Netherlands, where he is currently working toward the Ph.D. degree on the field of planar reflector phased array antenna for multiple applications.

Eduward Tangdiongga (S'01–M'10) received the M.Sc. and Ph.D. degrees from the Eindhoven University of Technology, The Netherlands, in 1994 and 2001, respectively. In 2001, he joined COBRA Research Institute working on ultrafast optical signal processing using semiconductor devices. In 2016, he was an Associate Professor on advanced optical access and local area networks. His current research interests include passive optical networks, radio over (single mode-, multimode-, and plastic) fiber, and optical wireless communication.

Bart Smolders (M'87–SM'07) received the M.Sc. and Ph.D. degrees in electrical engineering from the Eindhoven University of Technology, The Netherlands, in 1989 and 1994, respectively. He is a Full Professor since 2010 and currently the Dean of the Electrical Engineering Department, Eindhoven University of Technology. Until 2010, he has held applied research positions in industries including FEL-TNO, Thales Netherlands, The Netherlands Foundation for Research in Astronomy (ASTRON), and NXP (formerly Philips) Semiconductors. He is also the Chairman of the IEEE Benelux Section and the Chairman of the NERG (Nederlands Radio-en Elektronica Genootschap). His research interests include antenna systems and their application.

Ton Koonen (F'07) is a Full Professor in Eindhoven University of Technology since 2001. Since 2004, he has been the Chairman of the Group Electro-Optical Communication Systems and since 2012 the Vice-Dean of the Department of Electrical Engineering. Before 2001, he worked for more than 20 years in applied research in industry, among others in Bell Labs - Lucent Technologies. He is a Bell Labs Fellow (1998), an OSA Fellow (2013), and a Distinguished Guest Professor of Hunan University, Changsha, China, in 2014. In 2011, he received the Advanced Investigator Grant of the European Research Council. His current research interests include spatial division multiplexed systems, access and in-building fiber networks, including high-capacity POF networks, radio-over-fiber techniques and wireless optics techniques.